Advanced Synthesis & Catalysis

Accepted Article

Title: Strategic Approach on N-Oxides in Gold Catalysis – A Case Study

Authors: Jasmin Schießl, Philipp Stein, Judith Stirn, Kirsten Emler, Matthias Rudolph, Frank Rominger, and A. Stephen K. Hashmi

To be cited as: *Adv. Synth. Catal.* 10.1002/adsc.201801007

Link to VoR: http://dx.doi.org/10.1002/adsc.201801007

10.1002/adsc.201801007

VERY IMPORTANT PUBLICATION

Strategic Approach on *N*-Oxides in Gold Catalysis – A Case Study

Jasmin Schießl,[a] Philipp M. Stein,[a] Judith Stirn,[a] Kirsten Emler,[a] Matthias Rudolph,[a] Frank Rominger,[a] A. Stephen K. Hashmi[a,*]

a Organisch-Chemisches Institut, Heidelberg University, Im Neuenheimer Feld 270, 69120 Heidelberg, Germany.

E-mail: hashmi@hashmi.de

Abstract

An extensive kinetic study of selected key reactions of (oxidative) gold catalysis concentrates on the decrease of the catalytic activity due to inhibition of the gold(I) catalyst caused by pyridine derivatives that are obtained as by-products if *N*-oxides are applied as oxygen donors. The choice of the examined pyridine derivatives and their corresponding *N*-oxides has been made regardless of their commercial availability; particular attention has been paid to the practical benefit which up to now has been neglected in most of the reaction screenings. The test reactions were monitored by GC and ^{1}H NMR spectroscopy. The received reaction constants provide information concerning a correlation between the electronic structure of the heterocycle and the catalytic activity. Based on the collected kinetic data, it was possible to develop a basic set of three *N*-oxides which have to be taken into account in further oxidative gold(I)-catalyzed reactions.

Keywords

N-oxides; alkynes; kinetic studies; reaction optimization; catalyst inhibition; gold catalysis

Introduction

The impact of homogeneous gold catalysis increased over the last decades.[1] Since 2010,[2] gold-catalyzed oxidative cyclizations based on α-oxo-carbenoids generated by

10.1002/adsc.201801007

the attack of heteroaromatic *N*-oxides onto π-activated alkynes became one of the moist fruitful reaction classes in the field of gold catalysis.[3] Triggered by this reactivity pattern demanding transformations such as C-H insertions, cyclopropanations and ylide formations were enabled which provide an attractive replacement of α-diazo carbonyl compounds that were formerly used as precursors for α-oxo-carbenoids.[4] The quest for finding a suitable *N*-oxide for an oxidative gold-catalyzed transformation is often not easy as the pyridine by-products can lead to catalyst deactivation at higher conversions of the starting materials.[5] Interestingly despite this task, the reported choices of *N*-oxides merely depend on its commercial availability, despite the usually simple accessibility of *N*-oxides. This becomes obvious by an analysis of publications concerning experimental studies on this topic published from 2010 to 2018 (46 publications at 11.06.2018, Scifinder, keyword: gold catalysis *N*-oxide; only experimental studies are included). In sum, 32 different *N*-oxides were investigated. Overall, the average number of screened *N*-oxides is 4.2 per publication. 50 % of these publications deal with the oxidants like pyridine *N*-oxide, 3,5-dichloropyridine *N*-oxide or 8-methylquinoline *N*-oxide. 2-Bromopyridine *N*-oxide, 2,6-dibromopyridine *N*-oxide, 2,6-dichloropyridine *N*-oxide, 4-methylpyridine *N*-oxide or 8-isopropylquinoline *N*-oxide is only used in 20 % of the reports. One or more of the remaining 24 *N*-oxides were investigated in less than 10 % of these publications. This analysis shows that the choice of *N*-oxide is mostly based on its commercial availability and not on its practical benefit. Already published experimental data[3c,6] and mechanistic studies[7] report that the efficiency of the formation of the α-oxo gold carbenoid on basis of *N*-oxides is significantly affected by the formation of unavoidable by-products that can deactivate the active gold(I) species. Regarding this matter, Gagosz et al. postulated a series of potential equilibria which affect the activated gold species.[5] Especially, the deactivation of catalyst caused by the coordination of the pyridine *N*-oxide and the corresponding pyridine is significant. Without any doubt, a systematic investigation of the *N*-oxide influence on oxidative gold catalysis is needed. This encouraged us to shed light on the kinetics of these transformations as well as the significance of not yet or rarely applied *N*-oxides in homogeneous gold catalysis; regardless of their commercial availability. It should be noted that acid-assisted gold(I)-catalyzed reactions are not part of this analysis, however, of a different and still ongoing study.

10.1002/adsc.201801007

Results and Discussion

As an entry point, the dependency of the inhibition of the gold(I) catalyst on different pyridine derivatives was examined. To accomplish this, various pyridine gold(I) complexes and one *N*-methylmorpholine gold(I) complex were initially isolated. Noteworthy, only a few known pyridine gold(I) complexes are published to date.[8] For an effective synthesis, one equivalent of the gold(I) complex $Ph_3PAuNTf_2$ ([Au] = 0.034 mmol/ml) was treated with one equivalent of a pyridine derivative in DCM at 25 °C for 3 h (Scheme 1). With respect to the pyridine derivatives, representatives of commonly used *N*-oxides and pyridines which are characterized by varying electronic or steric effects were chosen. A precise ratio of the reactants turned out to be crucial as column chromatography was impossible due to the decomposition of the complex. After purification by recrystallization, the gold(I) complexes **1a-r** were obtained in excellent yields (85 – 100 %). However, the use of dihalogenated pyridines such as 2,5-/ 2,6-/ 3,5-dibromopyridine and 3,5-dichloropyridine did not afford the desired pyridine gold(I) complex, only the starting material was regained. These pyridines might be too electron-deficient to form a stable coordinative bond to the gold(I) center, so the coordination of the counter anion NTf_2^- is favored. Interestingly, Shi et al. isolated a pyridine gold(I) complex based on $Ph_3PAuSbF_6$ and 3,5-dibromopyridine.[8c]

10.1002/adsc.201801007

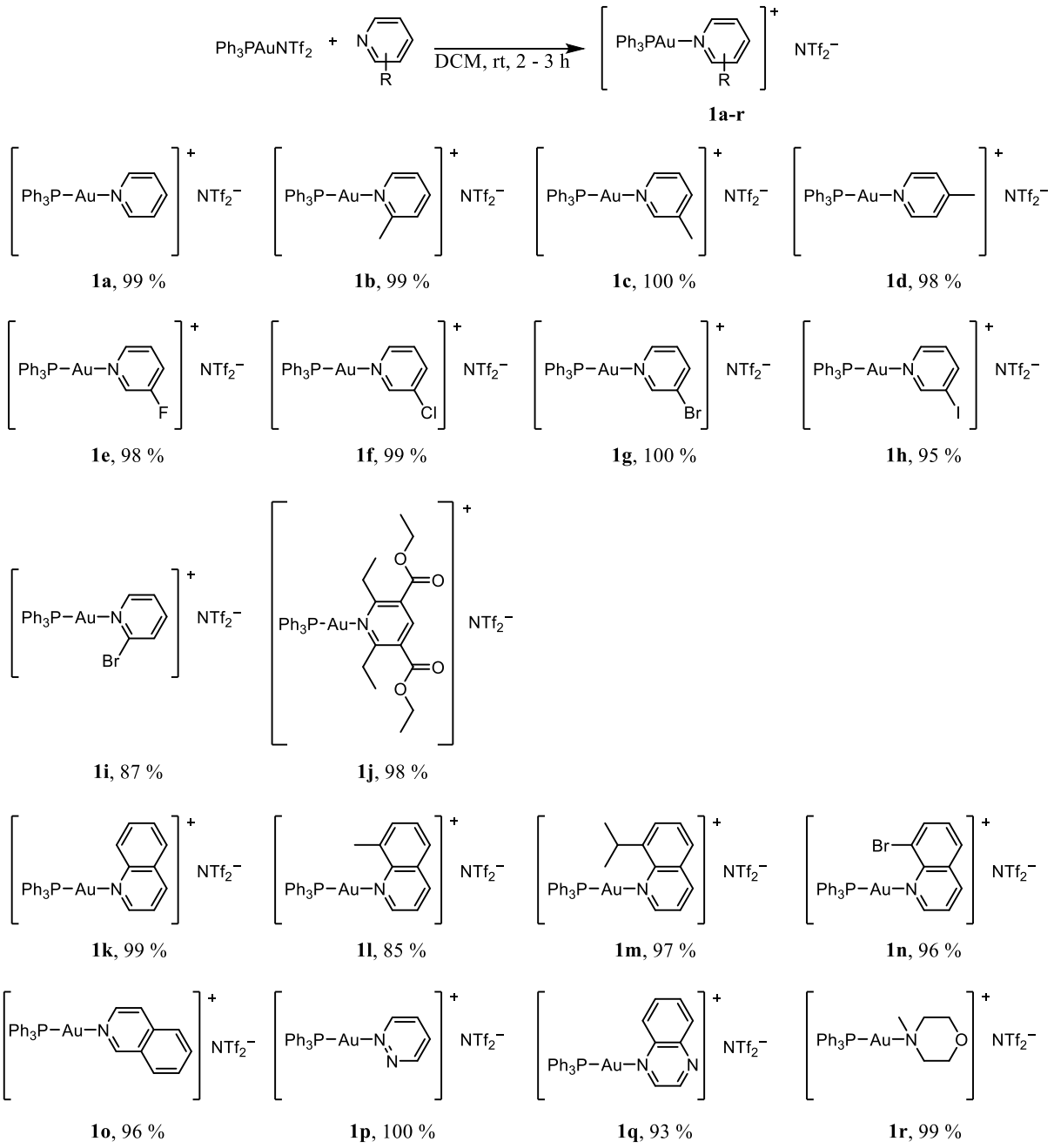

Scheme 1. Synthesis of gold(I) complexes coordinated by *N*-heterocycles

For some of the unknown structures, single crystal X-ray structures analyses were conducted (Figure 1); in Table 1 the structural parameters are summarized.[9] The gold(I) complexes differ only slightly in the selected Au–P and Au–N bond lengths and the solid state molecular structures of the gold(I) complexes **1k**, **1l**, **1n** and **1r** allow no conclusions concerning their behavior in solution.

10.1002/adsc.201801007

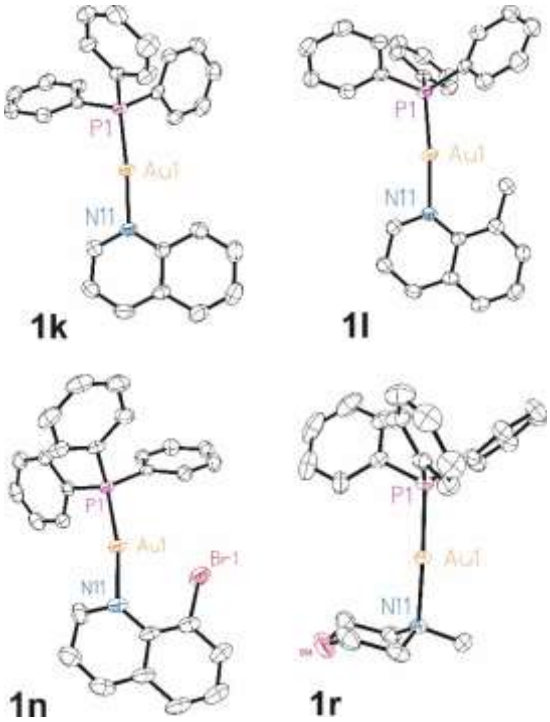

Figure 1. Solid state molecular structures of the gold(I) complexes **1k**, **1l**, **1n**, **1r**.

Table 1. Selected bond lengths and angles of the gold(I) complexes.

Gold(I) complex	Au–P [Å]	Au–N [Å]	P–Au–N [°]
1k	2.235 (10)	2.082 (3)	175.27 (10)
1l	2.234 (6)	2.104 (19)	174.38 (6)
1n	2.231 (11)	2.116 (4)	169.51 (13)
1r	2.240 (9)	2.127 (3)	177.70 (8)

Hereinafter, the catalytic activity of the isolated pyridine gold(I) complexes and accompanying the deactivation of the activated gold(I) species $Ph_3PAuNTf_2$ was examined on the basis of the literature-known cyclopropanation of styrene by a progargyl pivalate as a test reaction.[10] One advantage of the cyclopropanation reaction is certainly the remarkable rapid reaction time if $Ph_3PAuNTf_2$ is used as catalyst. In case of 5 mol% $Ph_3PAuNTf_2$, a complete conversion was obtained in less than 15 seconds; using 0.5 mol% in 4.5 minutes. A potentially significantly decreased rate constant using a pyridine gold(I) complex instead of $Ph_3PAuNTf_2$ still allows the examination of the reaction by means of common analysis methods. The kinetic investigations observed by GC were implemented by a standardized procedure (see

the Supporting Information for further details). Therefore, one equivalent of propargyl pivalate was treated with four equivalents of freshly distilled styrene and 5 mol% of the nitrogen coordinated gold(I) complex using *n*-dodecane as internal standard in DCM at 25 °C (Scheme 2). The reaction mixture was stirred with a speed of 400 rpm. To stop the reaction at a certain point of time, the separation of the catalyst was achieved by filtration through a short column of silica gel and the samples were analyzed by GC.

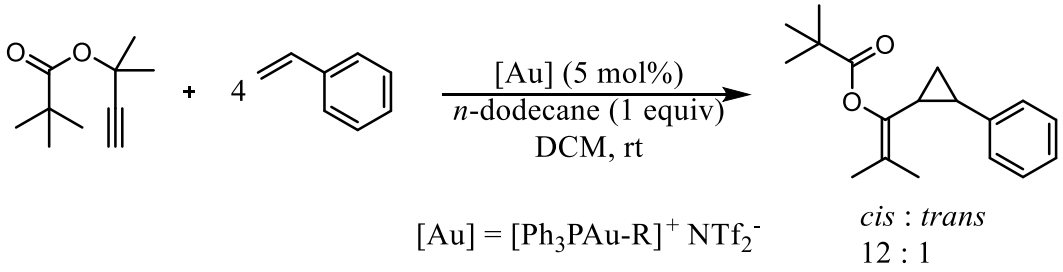

[2-Methylbut-3-yn-2-yl pivalate] = 0.0708 mmol/ml

Scheme 2. Gold(I)-catalyzed cyclopropanation of styrene with a propargyl pivalate.

The method of internal standard was used to improve the precision of quantitative analysis.[11] The integration method[12] confirmed the initially assumed second order reaction. As a result of graphic correlation, the rate constant was determined by standard kinetic methods. The calculated error is a result of error propagation of random faults caused by sample preparation. Systematic errors arising from the influence on the measurement object by instrument were excluded. The coefficient of determination R^2, a criterion to qualify a linear relation, expresses the goodness-of-fit of a regression if the coefficient is close to one. The results of the kinetic measurements are represented in Table 2. By way of illustration, the nitrogen coordinated gold(I) complexes are sorted by descending catalytic activity. Obviously, there are significant differences concerning the catalytic activity of various pyridine gold(I) complexes. In order to allow a better comparison, the relative rate constant k_{rel} of the unsubstituted pyridine gold(I) complex **1a** was normalized to $k_{rel} = 1$.

Table 2. Rate constants of the gold(I)-catalyzed cyclopropanation.[a]

10.1002/adsc.201801007

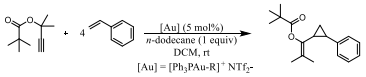

Entry	R=		k [L/(mol*h)]	R^2	k_{rel}
1		*in situ*	4607 ± 67	0.996	10194 ± 321
2		*in situ*	3068 ± 382	0.985	6788 ± 866
3		*in situ*	1114 ± 34	0.997	2465 ± 102
4		*in situ*	796 ± 31	0.995	1760 ± 85
5		*in situ*	461 ± 74	0.951	1020 ± 166
6		*in situ*	360 ± 43	0.973	796 ± 98
7		isolated	274 ± 14	1.000	606 ± 36
8		*in situ*	254 ± 12	0.994	562 ± 30
9		*in situ*	241 ± 19	0.966	532 ± 44
10		*in situ*	153 ± 5	0.990	338 ± 15
11		*in situ*	111 ± 3	0.998	245 ± 10
12		*in situ*	100 ± 6	0.992	221 ± 15
13		*in situ*	66.9 ± 1.2	0.999	148 ± 5
14		isolated	9.43 ± 0.37	0.985	20.9 ± 1.0
15		isolated	8.03 ± 0.22	0.996	17.8 ± 0.7
16		isolated	7.83 ± 0.44	0.966	17.3 ± 1.1
17		isolated	5.68 ± 0.15	0.993	12.6 ± 0.5
18		*in situ*	4.60 ± 0.20	0.981	10.2 ± 0.5
19		isolated	4.46 ± 0.16	0.986	9.86 ± 0.46
20		*in situ*	3.70 ± 0.35	0.855	8.19 ± 0.81
21	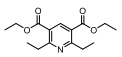	isolated	3.35 ± 0.11	0.988	7.41 ± 0.32
22		isolated	0.562 ± 0.026	0.977	1.24 ± 0.07
23		isolated	0.452 ± 0.013	0.982	1.00 ± 0.04
24		*in situ*	0.395 ± 0.012	0.979	0.875 ± 0.036
25		isolated	0.393 ± 0.012	0.989	0.869 ± 0.036
26		isolated	0.384 ± 0.012	0.979	0.850 ± 0.036
27		*in situ*	0.266 ± 0.010	0.984	0.588 ± 0.027
28		isolated	0.237 ± 0.011	0.963	0.524 ± 0.029
29		isolated	0.217 ± 0.009	0.957	0.479 ± 0.024
30		isolated	0.213 ± 0.012	0.955	0.470 ± 0.030
31		*in situ*	0.207 ± 0.010	0.934	0.458 ± 0.026
32		*in situ*	0.139 ± 0.016	0.869	0.308 ± 0.036
33		*in situ*	0.138 ± 0.008	0.909	0.305 ± 0.020
34		*in situ*	0.134 ± 0.013	0.878	0.297 ± 0.030
35		*in situ*	0.035 ± 0.008	0.848	0.078 ± 0.019
36		isolated	0.014 ± 0.009	0.070	0.030 ± 0.021

[a] *Reaction conditions:* propargyl pivalate (150.9 µmol, 70.8 µmol/ml), styrene (603.7 µmol), *n*-dodecane (150.9 µmol), pyridine derivative (5 mol%; if *in situ*), gold(I) catalyst (5 mol%), DCM at T = 25 °C, observed by GC monitoring for up to 5 h.

In the first instance, the comparability of isolated and *in situ* generated pyridine gold(I) complexes was examined. As an example serves the reaction of the pre-prepared gold(I) complex **1n** (Table 2; entry 19) and the reaction of $Ph_3PAuNTf_2$ in combination with 8-bromoquinoline in a ratio of 1:1 (Table 2; entry 18) due to the extended reaction time up to several hours (Figure 2). Obviously, both procedures lead to a comparable reaction progress. Besides, the calculated rate constants k are consistent within the error tolerances. The kinetic investigation using the heterocycle 2-bromopyridine confirm this observation (Table 2; entries 7 and 9). It is evident, therefore, that the reaction behavior is independent of the usage of isolated or *in situ* generated gold(I) complexes.

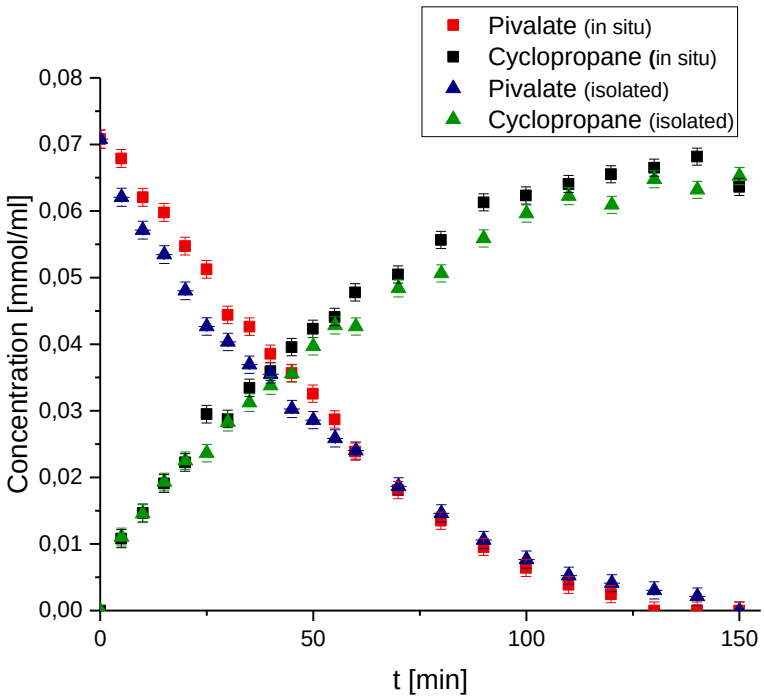

Figure 2. Direct comparison of the cyclopropanation of styrene with a propargyl pivalate using the isolated and the *in situ* generated 8-bromoquinoline gold(I) complex.

In a first set of experiments differently-substituted pyridine derivatives bearing one or more electron-withdrawing substituents were converted (Table 2; entries 1 – 10, 13 – 19). Unexceptionally, a significantly increased catalytic activity was obtained compared to the gold(I) complexes of the unsubstituted pyridine (Table 2; entry 23) and quinoline

10.1002/adsc.201801007

(Table 2; entry 22). Especially, the addition of pentafluoropyridine yielded an extraordinarily high catalytic activity (Table 2; entry 1). A complete conversion was already observed after a reaction time of 30 seconds, however, the reaction is still more than two times slower than the reaction using $Ph_3PAuNTf_2$ without additives. An enhanced catalytic activity correlates with the amount of halide substituents (Table 2; entries 1 – 3, 5 – 7). Additionally, the catalytic activity of halogenated pyridine derivatives declines with a lower electronegativity of the halide (Table 2; entries 14 – 17). Furthermore, the substitution pattern of the pyridine derivatives affects the catalytic activity. In case of bromopyridines as well as dibromopyridines, the 2-substituted or rather 2,6-disubstituted pyridine derivatives (Table 2; entries 2, 9) show a higher rate constant than the 3-substituted or 3,5-disubstituted isomers (Table 2; entries 6, 15). As expected, the catalytic activity of the 2,5-dibromopyridine derivative (Table 2; entry 3) is decreased compared to the 2,6-dibrominated analogue and increased in comparison to the 3,5-dibrominated isomer. Significantly reduced rate constants were obtained by using pyridine derivatives including exclusively electron-donating substituents (Table 2; entries 24 – 29, 31, 33 – 35). In case of electron-donating substituents the catalytic activity is up to ten times lower than using the unsubstituted analogues. Pyridine derivatives with increased σ-donor properties caused by an enhanced electron density of the heterocycle form a stable coordinative bond to the gold(I) center. As a consequence, the dissociation of the pyridine gold(I) complex occurs in low probability. This becomes particularly obvious in case of 2,6-di-*tert*-butyl-4-methylpyridine as additive (Table 2; entry 34), here, the reaction rate is more than three times lower than using the unsubstituted pyridine. Interestingly, the steric effects are not as pronounced as the electronic effects. A comparison of the additives 2,6-di-*tert*-butyl-4-methylpyridine, 2,6-di-*tert*-butylpyridine and 2-methylpyridine clearly demonstrates this (Table 2; entries 27, 28, 34). In case of electron-donating substituents, the substituent pattern is not that pronounced. Independent of the position, the rate constants of the methyl-substituted pyridine derivatives coincide within the error tolerances (Table 2, entries 28, 29, 31). The quinoline gold(I) complexes are characterized by a similar trend as the pyridine derivatives. The catalytic activity decreases with an enhanced electron density of the nitrogen atom. The different reactivity of the unsubstituted pyridine derivative's gold(I) complex is caused by varying basicity (Table 2; entries 22, 23, 30, 32). Due to the *peri* steric effect,[13] a higher basicity is expected for acridine, quinoline and isoquinoline in

10.1002/adsc.201801007

comparison to pyridine. The basicity order is acridine > isoquinoline > pyridine > quinoline. Obviously, pyridine derivatives with an increased basicity show a lower reactivity. The notably declined catalytic activity of the acridine derivative confirms this hypothesis (Table 2; entry 32). In comparison to pyridine derivatives, diazines have a lower electron density due to a further electron withdrawing nitrogen atom. As a result, an increased catalytic activity was observed by using diazine gold(I) complexes (Table 2; entry 11, 12, 20). *N*-Methylmorpholine was investigated as an exceptional aliphatic heterocycle (Table 2; entry 36). Within a reaction time of two days, only a low conversion was observed.

Nevertheless, in case of oxidative gold catalysis using *N*-oxides up to one equivalent of the corresponding pyridine derivative exists in the reaction mixture at late reaction states. Therefore, in a second set of experiments, the influence of the pyridine derivative concentration was examined (Table 3). Due to its relatively high reaction rate in case of 5 mol% pyridine derivative, 2-bromopyridine in combination with the gold catalyst $Ph_3PAuNTf_2$ was chosen for further investigations. As expected, the catalytic activity of the gold(I) complex significantly decreases in combination with an enhanced amount of 2-bromopyridine (Table 3; Figure 3). The graphic correlation of the rate constants depending on the equivalents of deployed 2-bromopyridine shows an interesting effect (Figure 4). An exponential dependence using various ratios of $Ph_3PAuNTf_2$ to pyridine derivative becomes obvious. This is caused by a slight equilibrium shift towards the pyridine gold(I) complex with increasing concentration of 2-bromopyridine.

Table 3. Influence of various 2-bromopyridine concentrations on the cyclopropanation.

10.1002/adsc.201801007

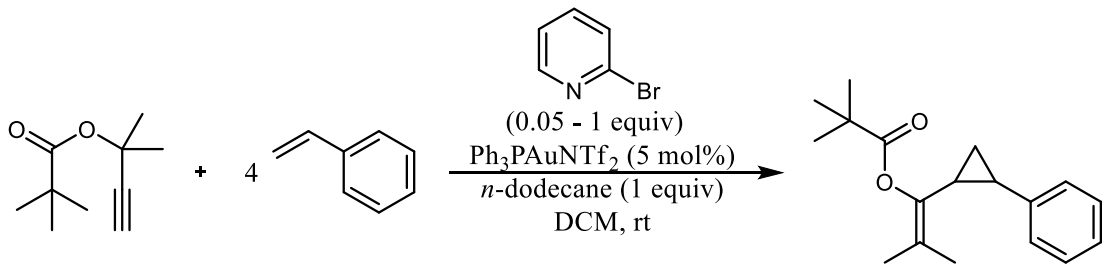

Entry	Equivalents of 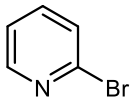	k [L/(mol*h)]	R^2	k_{rel}
1	0.05	241 ± 19	0.966	1.00 ± 0.11
2	0.10	40.4 ± 1.4	0.979	0.168 ± 0.014
3	0.15	22.8 ± 0.7	0.981	0.095 ± 0.008
4	0.20	20.5 ± 0.6	0.985	0.085 ± 0.007
5	0.25	13.1 ± 0.5	0.975	0.055 ± 0.005
6	0.50	10.1 ± 0.5	0.986	0.042 ± 0.004
7	1.00	3.35 ± 0.10	0.992	0.014 ± 0.001

10.1002/adsc.201801007

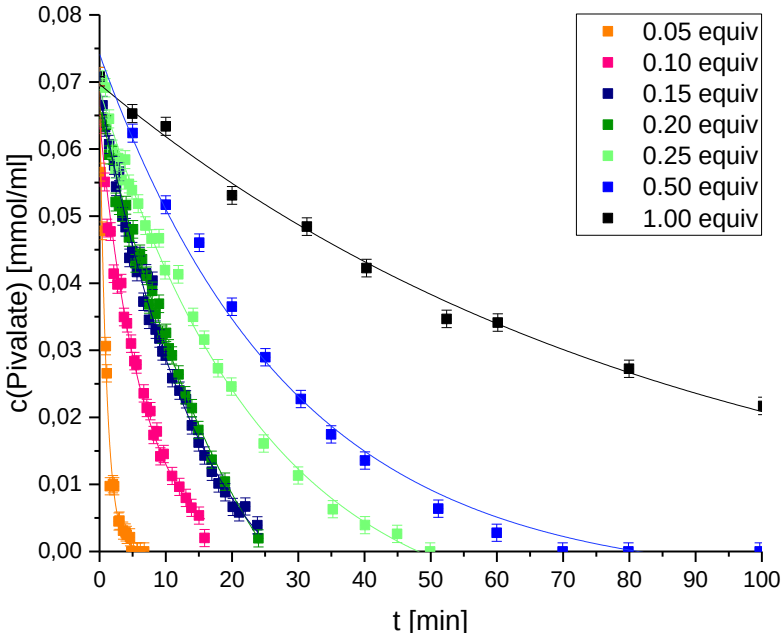

Figure 3. Decrease of the propargyl pivalate depending on the 2-bromopyridine concentration.

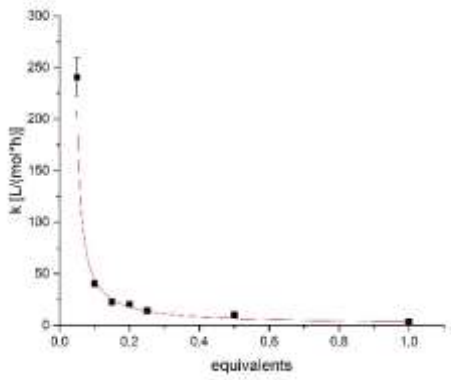

Figure 4. Exponential dependence of the rate constant.

In sum, the kinetic investigation of the cyclopropanation of styrene with a propargylic pivalate demonstrates that the electronic structure of the pyridine additive significantly affects the catalytic activity, whereas the steric effect is less pronounced. Moreover, the pyridine concentration is of considerable interest. These observations are crucial for the application of pyridine derivatives as organic bases and as starting materials in homogeneous gold catalysis. Due to insertion of defined substituents, it might be possible to predict and ultimately increase the reactivity.

Subsequently, further kinetic investigations were conducted on the basis of test reactions with commonly used or easily accessible *N*-oxides. The *N*-oxides were

synthesized according to literature procedure (see Supporting Information for further details).[14] However in case of the pyridine derivatives pentafluoropyridine, dimethyl pyridine-2,5-dicarboxylate, 2,6-di-*tert*-butyl-pyridine, 2,6-di-*tert*-butyl-4-methylpyridine, 8-bromoquinoline, common synthetic strategies[15] did not yield the desired product. Due to this, these *N*-oxides were excluded from further consideration. Initially, the literature-known oxazole synthesis introduced by Zhang's group was investigated as a test reaction.[16] The oxazole synthesis is not only a key reaction type in homogeneous gold catalysis, it also includes the application of easily accessible starting materials and has a suitable reaction time of a few hours. As in the case of the cyclopropanation reaction, the kinetic investigations were observed by GC using a standardized procedure to ensure the comparability (see the Supporting Information for further details). Therefore, one equivalent of phenylacetylene was treated with 1.3 equivalents of *N*-oxide, one equivalent of *n*-dodecane as internal standard and 5 mol% of $Ph_3PAuNTf_2$ in acetonitrile at 60 °C (Scheme 3). The reaction mixture was stirred with a speed of 400 rpm. Here again, samples of the reaction mixture were taken in time intervals adjusted to the reaction time. To abort the reaction at a certain point of time, the separation of the catalyst was gained by filtration through a short column of silica gel. Afterwards, the samples were analyzed by GC monitoring. The evaluation of the kinetic data was conducted in accordance with the analysis of the cyclopropanation. The integration method[12] proved the initially assumed pseudo second order reaction. Due to the fact that acetonitrile performs as reactant and solvent, the concentration of acetonitrile can be regarded as constant. The rate constant k* takes the acetonitrile concentration into account. In Table 4, the results of the kinetic measurements are shown. The experimental data was sorted by *N*-oxides with descending rate constants. An exemplary reaction progress is shown in Figure 5.

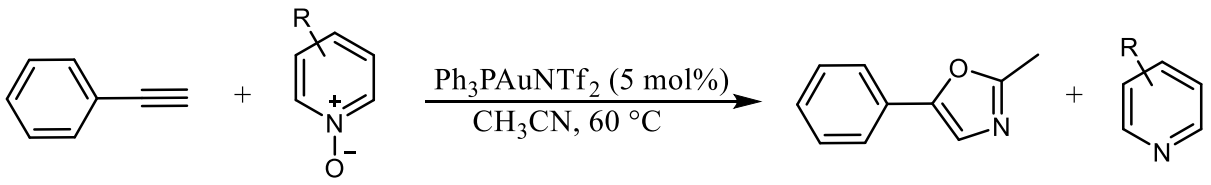

[Phenylacetylene] = 0.0967 mmol/ml

Scheme 3. Gold(I)-catalyzed oxazole synthesis.

Table 4. Rate constants of the gold(I)-catalyzed oxazole synthesis.[a]

10.1002/adsc.201801007

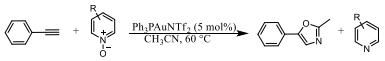

Entry	*N*-Oxide	Conversion [%] 2.5 h	Conversion [%] 24 h	k [L/(mol*h)]	k* [L²/(mol²*h)]	R^2	k_{rel}
1		66	78	43.1 ± 4.1	2.30 ± 0.22	0.979	6.96 ± 0.88
2		100	100	31.9 ± 2.1	1.71 ± 0.11	0.988	5.16 ± 0.54
3		62	100	31.9 ± 2.3	1.70 ± 0.12	0.995	5.15 ± 0.56
4		62	99	29.8 ± 2.7	1.60 ± 0.15	0.980	4.82 ± 0.60
5		31	50	29.2 ± 5.3	1.56 ± 0.32	0.985	4.71 ± 1.03
6		68	96	27.1 ± 2.0	1.45 ± 0.11	0.992	4.38 ± 0.49
7		62	90	20.6 ± 2.3	1.10 ± 0.12	0.958	3.32 ± 0.46
8		61	71	19.5 ± 1.5	1.05 ± 0.08	0.998	3.16 ± 0.35
9		57	81	15.8 ± 1.4	0.84 ± 0.07	0.983	2.54 ± 0.32
10		48	62	15.3 ± 1.5	0.81 ± 0.08	0.979	2.47 ± 0.32
11		68	98	14.4 ± 1.2	0.77 ± 0.06	0.974	2.33 ± 0.27
12		68	76	12.4 ± 1.0	0.67 ± 0.05	0.989	2.01 ± 0.23
13		80	100	12.3 ± 0.8	0.66 ± 0.04	0.990	1.99 ± 0.21
14		64	93	11.0 ± 0.8	0.59 ± 0.04	0.989	1.78 ± 0.20
15		56	-	9.90 ± 0.72	0.53 ± 0.04	0.994	1.60 ± 0.18
16		53	63	7.76 ± 0.66	0.42 ± 0.04	0.978	1.25 ± 0.15
17		60	100	6.19 ± 0.51	0.33 ± 0.03	0.984	1.00 ± 0.12
18		50	82	6.00 ± 0.54	0.32 ± 0.03	0.972	0.97 ± 0.12
19		22	80	5.16 ± 0.54	0.28 ± 0.03	0.974	0.83 ± 0.11
20		40	93	4.67 ± 0.35	0.25 ± 0.02	0.983	0.76 ± 0.08
21		26	-	3.59 ± 0.28	0.19 ± 0.02	0.973	0.58 ± 0.07
22		29	45	2.27 ± 0.28	0.12 ± 0.02	0.949	0.36 ± 0.05
23		35	90	2.05 ± 0.19	0.11 ± 0.01	0.971	0.33 ± 0.04
24		15	13	1.04 ± 0.09	0.056 ± 0.005	0.965	0.17 ± 0.02
25	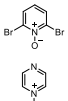	6	10	0.90 ± 0.12	0.05 ± 0.01	0.961	0.15 ± 0.02
26		16	34	0.64 ± 0.05	0.034 ± 0.003	0.964	0.10 ± 0.01
27		5	-	0.49 ± 0.05	0.026 ± 0.003	0.982	0.08 ± 0.01
28		9	-	0.14 ± 0.02	0.007 ± 0.001	0.969	0.022 ± 0.003
29		8	10	0.010 ± 0.002	0.00054 ± 0.00013	0.868	0.0016 ± 0.0004
30	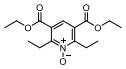	0.02	0.39	0.0017 ± 0.0001	0.000090 ± 0.0000064	0.996	0.00027 ± 0.00003

10.1002/adsc.201801007

[a] *Reaction conditions:* phenylacetylene (0.30 mmol, 0.0967 mmol/ml), *N*-oxide (0.39 mmol), *n*-dodecane (0.30 mmol), $Ph_3PAuNTf_2$ (5 mol%), acetonitrile at T = 60 °C, observed by GC monitoring for up to 5 h.

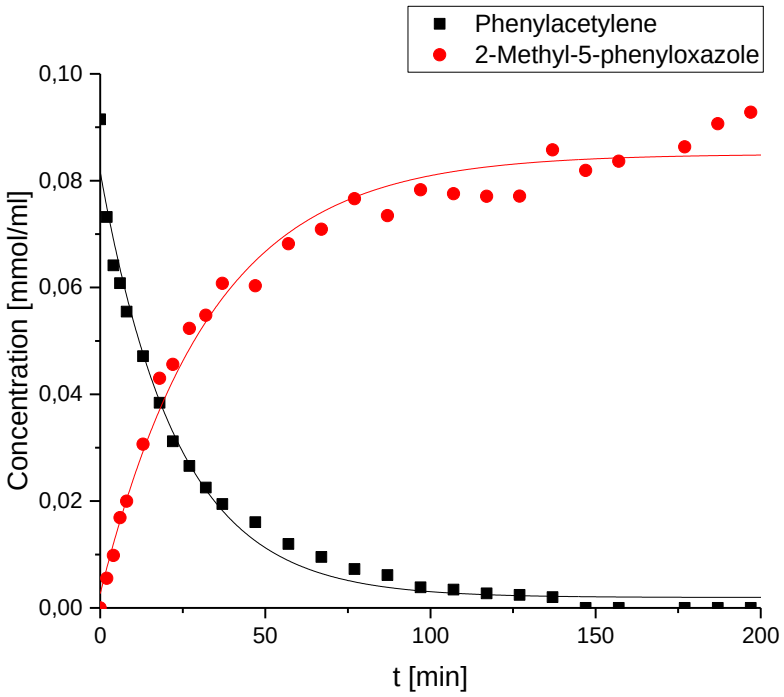

Figure 5. Exemplary oxazole synthesis using 8-methylquinoline *N*-oxide (Table 4; entry 2).

The initial kinetic investigation of differently substituted pyridine *N*-oxides with one or more electron-withdrawing substituents show up to seven times increased reactivity than using the unsubstituted analogue (Table 4; entries 1, 3 – 12, 15). Exclusively, the 2,6-dibromopyridine *N*-oxide performed worse than first expected (Table 4; entry 25). 2,5-dibromopyridine *N*-oxide achieved the highest reactivity by far (Table 4; entry 1), however, the application of dihalogenated *N*-oxides did not lead to a full conversion after a reaction time of 24 h (Table 4; entries 1, 6, 7). As mentioned in connection with the cyclopropanation, the enhanced reactivity correlates with the amount of halide substituents (Table 4; entries 1, 6 – 9). In case of the monohalogenated pyridine *N*-oxides, a strong dependence of the electronegativity on the reactivity becomes obvious (Table 4; entries 3, 4, 9, 11). It clearly demonstrates that substituents with an increased electronegativity obtain a higher reaction rate. The only exception is shown by using the dihalogenated pyridine *N*-oxides (Table 4; entries 6, 7). Here, the rate constants are nearly consistent within the error tolerances. This is caused by the slight difference in electronegativity of bromine and chlorine. Additionally, the substitution pattern of the

10.1002/adsc.201801007

pyridine *N*-oxide affect the reactivity. Independent of electron-withdrawing (Table; entries 8, 9) or donating substituents (Table 4; entries 20, 21, 27), substituents in 2-position gain a higher reaction constant than their 3-substituted isomer; 4-substituted derivatives show by far the worst reactivity. With the exception of 2,6-dibromopyridine *N*-oxide, this observation is also transferable to the dibrominated *N*-oxides (Table 4; entries 1, 6). Due to the negative inductive effect of the CF_3- and CHF_2-substituents, the corresponding *N*-oxides achieved a more than two times higher rate constant than the unsubstituted analogue (Table 4; entries 10, 12). As expected, pyridine *N*-oxides including solely electron-donating substituents lead to significantly decreased reaction rates (Table 4; entries 16, 20 – 22, 27, 28). The introduction of an electron-donating substituent increases the N–O bond length and considerably enhances the electron density on the oxygen. Furthermore, *N*-oxides with electron donating substituents show a greater complexation ability than *N*-oxides with electron-withdrawing substituents. Belova et al. confirm this expectation by DFT calculations.[17] The Hantzsch ester *N*-oxide nearly yielded no consumption (Table 4; entry 30). After a reaction time of 72 h, only 1 % of the phenylacetylene was converted. The application of substituted quinoline *N*-oxides showed different trends than the pyridine derivatives. 8-Methylquinoline *N*-oxide gained a three times higher reaction constant than unsubstituted quinoline *N*-oxide (Table 4; entries 2, 14). The reaction using 8-isopropylquinoline *N*-oxide is characterized by a decreased reaction rate (Table 4; entry 13). An outstanding high reactivity was estimated using 8-iodoquinoline *N*-oxide (Table 4; entry 5), however, the *N*-oxide did not meet the expectations. With one exception, the rate constants of *N*-oxides of the pyridine derivatives quinoline, pyridine, isoquinoline and acridine are consistent with the basicity order; the higher the basicity, the lower the reactivity (Table 4; entries 14, 17, 19, 23). Although a further electron-withdrawing nitrogen atom decreases the electron density, the diazine *N*-oxides perform worse than the *N*-oxide of pyridine or quinoline (Table 4; entries 18, 24, 26). The aliphatic *N*-methylmorpholine manifested in penultimate place (Table 4; entry 29).

To confirm the examined trends, the set of *N*-oxides was investigated by means of another literature-known key reaction type in gold catalysis, an oxidative ring expansion. Here, the synthesis of a functionalized tropone derivative serves as a test reaction.[18] Due to the higher resolution in time of NMR kinetics, the kinetic investigations were conducted by *in situ* monitoring with ^{1}H NMR spectroscopy at 25 °C (see the Supporting Information for further details). The use of a continuous

measurement enables the recording of 256 ^{1}H NMR spectra within a period of maximum twelve hours. The sample composition consists of one equivalent of alkynyl quinol, 1.3 equivalents of *N*-oxide and 5 mol% $Ph_3PAuNTf_2$ in deuterated DCM (Scheme 4). Due to the *in situ* monitoring, the use of an internal standard is not necessary.

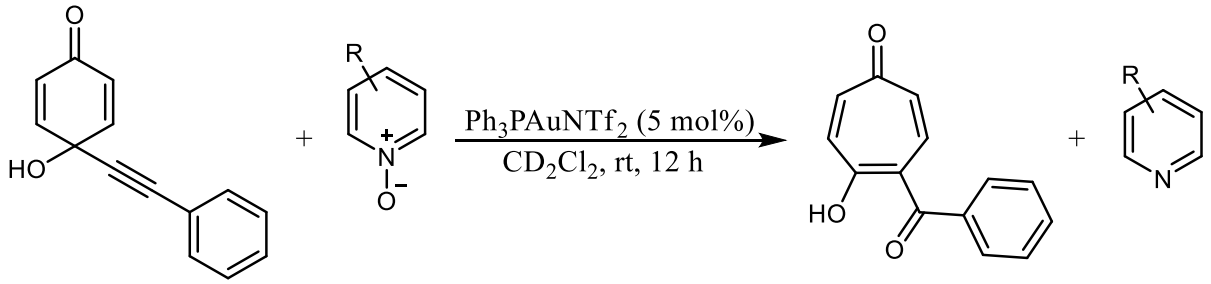

[4-Hydroxy-4-(phenylethynyl)cyclohexa-2,5-dien-1-one] = 0.10 mmol/ml

Scheme 4. Gold(I)-catalyzed oxidative ring expansion of an alkynyl quinol.

Analogous to the analysis of the cyclopropanation and the oxazole synthesis, the evaluation of the kinetic data was implemented. The integration method[12] serves for the determination of the reaction order. Once more, this procedure confirmed the initially assumed second order reaction. The results of the kinetic investigations are summarized in Table 5, whereby the rate constants of the *N*-oxides are sorted in descending order. As observed before, there are substantial differences concerning the reactivity of the *N*-oxides. An exemplary reaction progress is shown in Figure 6.

Table 5. Rate constants of the gold(I)-catalyzed oxidative ring expansion of an alkynyl quinol.[a]

10.1002/adsc.201801007

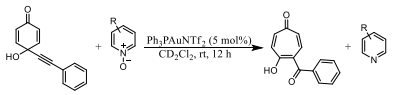

Entry	*N*-Oxide	k [L/(mol*h)]	R^2	k_{rel}
1		207 ± 14	0.997	374 ± 33
2		147 ± 9	0.996	267 ± 22
3		47.2 ± 2.4	0.999	85.4 ± 6.5
4		47.2 ± 2.5	0.998	85.4 ± 6.6
5		24.9 ± 1.3	0.998	45.1 ± 3.5
6		21.6 ± 1.1	0.994	39.0 ± 1.0
7		15.7 ± 0.8	0.998	28.4 ± 2.2
8		6.85 ± 0.34	0.998	12.4 ± 0.9
9		6.32 ± 0.32	0.999	11.4 ± 0.9
10		6.00 ± 0.30	0.998	10.9 ± 0.8
11		2.57 ± 0.13	0.997	4.65 ± 0.35
12		2.53 ± 0.13	0.997	4.57 ± 0.35
13		2.47 ± 0.14	0.996	4.47 ± 0.35
14		2.31 ± 0.13	0.997	4.19 ± 0.34
15		2.20 ± 0.11	0.998	3.99 ± 0.30
16		1.65 ± 0.09	0.995	2.99 ± 0.23
17		1.34 ± 0.07	0.998	2.42 ± 0.18
18		1.06 ± 0.06	0.997	1.92 ± 0.15
19		0.827 ± 0.045	1.000	1.50 ± 0.12
20		0.778 ± 0.041	0.994	1.41 ± 0.11
21		0.761 ± 0.043	0.993	1.38 ± 0.11
22		0.553 ± 0.031	0.998	1.00 ± 0.08
23		0.493 ± 0.025	0.996	0.892 ± 0.068
24		0.349 ± 0.019	0.997	0.632 ± 0.049
25		0.232 ± 0.013	0.999	0.420 ± 0.033
26		0.183 ± 0.10	0.992	0.332 ± 0.026
27		0.174 ± 0.010	0.995	0.315 ± 0.025
28		0.137 ± 0.007	0.998	0.248 ± 0.019
29		0.064 ± 0.003	0.994	0.116 ± 0.009
30	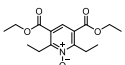		no reaction	

10.1002/adsc.201801007

[a] *Reaction conditions:* alkynyl quinol (0.060 mmol, 0.10 mmol/ml), *N*-oxide (0.078 mmol), $Ph_3PAuNTf_2$ (5 mol%), deuterated DCM at T = 25 °C, observed by ^1H NMR monitoring for up to 12 h.

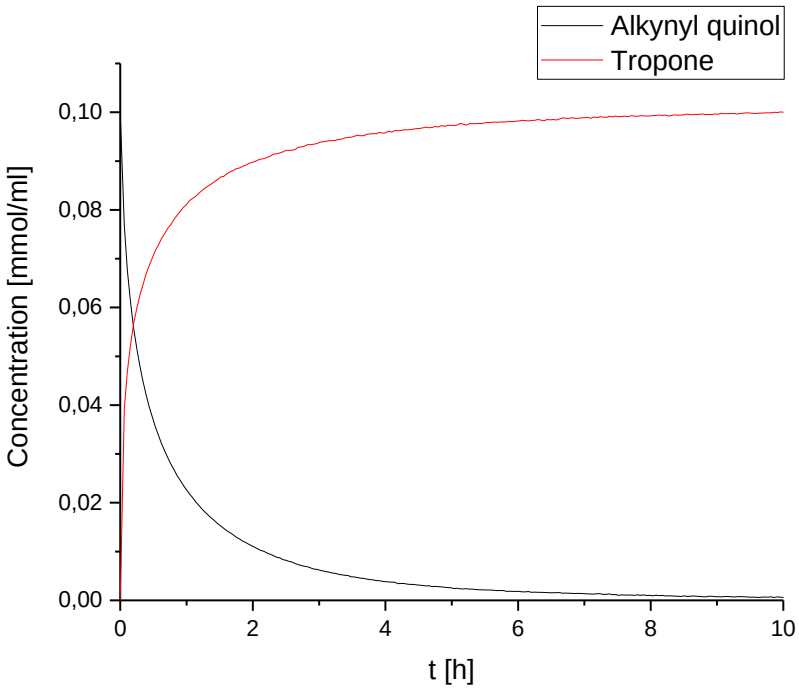

Figure 6. Exemplary oxidative ring expansion using 3,5-dibromopyridine *N*-oxide (Table 5; entry 5).

The kinetic investigations clearly show a dependence of the electronic effect caused by differently substituted pyridine *N*-oxides on the reactivity. Pyridine *N*-oxides with one or more electron withdrawing substituents show more than eighty times higher rate constants than the unsubstituted analogue (Table 5; entries 3 – 5, 7 – 14, 20). The decrease of electron density using an enhanced amount of halide substituents leads to an increased reactivity. Exclusively, the 2,6-dibromopyridine *N*-oxide performed worse (Table 5; entry 8). Different monohalogenated pyridine *N*-oxides yielded the same rate constants within the error tolerances (Table 5; entries 11 – 14). Here, the electronegativity is not affecting the reactivity. However, a dependence of the substitution pattern of the pyridine *N*-oxides on the rate constants was observed. Electron-withdrawing substituents in 2-position achieved a higher reaction rate than the 3-substituted isomer (Table 5; entries 7, 12). Interestingly, in case of electron-donating substituents a reverse effect was monitored (Table 5; entries 19, 21, 24). Pyridine *N*-oxides containing electron donating substituents (Table 5; entries 15, 16, 19, 21, 24, 26) yielded a significantly lower reactivity compared to the *N*-oxides with

10.1002/adsc.201801007

electron-withdrawing substituents, however, not necessarily lower than the unsubstituted pyridine *N*-oxide. The application of the Hantzsch ester *N*-oxide did not afford a reaction (Table 5; entry 30). As observed in case of the oxazole synthesis, the substituted quinoline *N*-oxides exhibited different trends than the pyridine derivatives. 8-Isopropylquinoline *N*-oxide achieved the highest rate constant by far, closely followed by 8-methylquinoline *N*-oxide (Table 5; entries 1, 2). The use of 8-iodoquinoline *N*-oxide promised an outstanding high reactivity, however, the *N*-oxide did not meet the expectations (Table 5; entry 6). The reactivity of the *N*-oxides of the pyridine derivatives quinoline, isoquinoline, pyridine and acridine exclusively are in accordance with the basicity order (Table 5; entries 17, 22, 23, 28). Thereby, the acridine *N*-oxide which possesses the highest basicity in this series afforded the lowest rate constant. The diazine *N*-oxides obtained a lower reaction rate than the *N*-oxide of pyridine and quinoline (Table 5; entries 18, 25, 27). In accordance with the oxazole synthesis, the aliphatic *N*-methylmorpholine gained the penultimate place (Table 5; entry 29).

The kinetic studies of the oxazole synthesis and the oxidative ring expansion show a definite trend concerning the necessary electronic properties of the *N*-oxides. Interestingly, one of the best *N*-oxides, the 2,5-dibromopyridine *N*-oxide, was not used in literature before. Although the synthesis of the 2,5-dibromopyridine *N*-oxide is as simple as for every other *N*-oxide as well. The use of 2,5-dibromopyridine *N*-oxide in further oxidative gold(I)-catalyzed reactions shall ensure the transferability of the results. Thereby, a comparison to already published results was aimed. Therefore, the general procedure is in accordance to literature to guarantee a comparability of the obtained results. Hence, the literature-known synthesis of indenone was examined.[19] One equivalent of 1,5-diyne was treated with 1.5 equivalents of *N*-oxide and 5 mol% $Ph_3PAuNTf_2$ in deuterated acetonitrile at 60 °C. Hexamethylbenzene was used as internal standard for ^1H NMR-monitoring. The results are shown in Table 6. As expected the 2,5-dibromopyridine *N*-oxide significantly improves the reaction. The highest published yield (58 %) was achieved by 8-ethylquinoline *N*-oxide after a reaction time of 17 hours. In case of 2,5-dibromopyridine *N*-oxide a complete consumption and additionally a quantitative yield were monitored after even 30 min.

Table 6. Gold(I)-catalyzed cyclization of 1,5-diyne.[a]

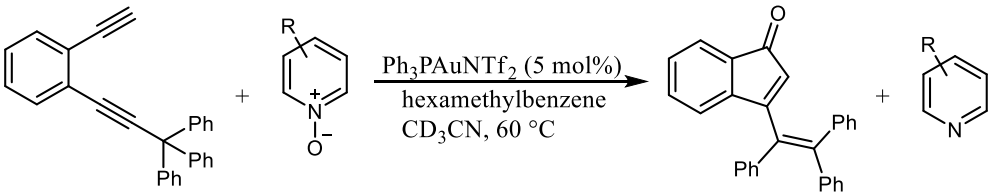

[(3-(2-Ethynylphenyl)prop-2-yne-1,1,1-triyl)tribenzene] = 0.292 mmol/ml

***N*-Oxide**	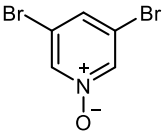	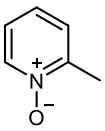	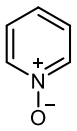	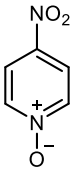	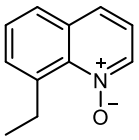	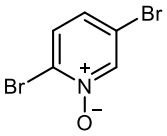
Yield [%]	47	45	51	31	58	100[b]

[a] *Reaction conditions:* 1,5-diyne (0.140 mmol, 0.292 mmol/ml), *N*-oxide (0.210 mmol), hexamethylbenzene (0.016 mmol), $Ph_3PAuNTf_2$ (5 mol%), deuterated acetonitrile at T = 60 °C, observed by ^1H NMR monitoring for 17 h.

[b] Yield after a reaction time of 30 min.

Additionally, the oxidative cyclization of propynyl arene into indan-2-one was investigated.[5,20] Therefore, one equivalent of 3-phenyl-1-propyne was converted with 1.2 equivalents of *N*-oxide and 4 mol% $Ph_3PAuNTf_2$ in deuterated $CHCl_3$ at 20 °C. 1,4-Dinitrobenzene was used as internal standard for ^1H NMR monitoring. In Table 7, the conversion related to different reaction times is listed in a direct comparison of 2-(*tert*-butyl)-6-chloropyridine *N*-oxide and 2,5-dibromopyridine *N*-oxide. Although the reaction comes to a standstill after a reaction time of six hours, a nearly two times higher conversion was yielded by using 2,5-dibromopyridine *N*-oxide. 2-(*tert*-butyl)-6-chloropyridine *N*-oxide afforded the best results in the published reaction screening. It should be noted that further published results were achieved using a biarylphosphonite gold(I) complex. Due to this, further results are not comparable to this investigation.

Table 7. Gold(I)-catalyzed oxidative cyclization of propynyl arene into indan-2-one.[a]

10.1002/adsc.201801007

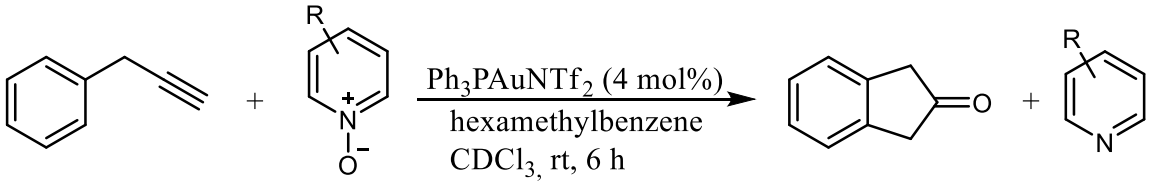

[Prop-2-yn-1-ylbenzene] = 0.20 mmol/ml

***N*-Oxide**	**Conversion [%]**			
	0.25 h	2 h	4 h	6 h
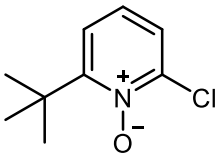	3	12	18	25
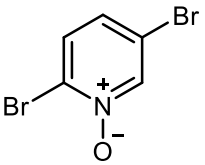	20	39	43	44

[a]

Reaction conditions: prop-2-yn-1-ylbenzene (0.12 mmol, 0.20 mmol/ml), *N*-oxide (0.24 mmol), hexamethylbenzene (0.027 mmol), $Ph_3PAuNTf_2$ (4 mol%), deuterated chloroform at T = 20 °C, observed by ^1H NMR -monitoring.

Conclusions

In an initial systematic kinetic study, the inhibition of the gold(I) catalyst by various pyridine derivatives was examined by means of a cyclopropanation reaction. Related to this a series of pyridine gold(I) complexes has been synthesized and evaluated by single crystal X-ray structure analyses. Comparison experiments have proven that the isolated and *in situ* generated pyridine gold(I) complexes achieve a similar catalytic activity. The electronic structure of these complexes significantly affects the catalytic activity. Pyridine derivatives with increased σ-donor properties caused by an enhanced electron density of the nitrogen atom of the heterocycle form a more stable coordinate bond to the Lewis-acidic gold(I) center, finally, the degree of inhibition rises. This trend became apparent in case of pyridine derivatives with different electronic properties and various substitution patterns. The influence of the pyridine concentration on the catalytic activity is noteworthy, an exponential dependence was observed. Especially, these results are of major importance for the transfer to other applications. The insertion of defined substituents to selected pyridine derivatives which might be applied

10.1002/adsc.201801007

for example as organic base or starting material possibly increase the reactivity. Moreover, a detailed kinetic study of two key reactivity types of oxidative gold catalysis using yet unapplied or only rarely applied *N*-oxides, regardless of their commercial availability, was conducted. For both test reactions, similar reaction trends – apart from a few exceptions – in accordance with the results of the cyclopropanation were observed. In all cases, outstanding results were achieved using 2,5-dibromopyridine *N*-oxide and 8-methylquinoline *N*-oxide. The practical benefit of 2,5-dibromopyridine *N*-oxide is additionally shown by the exemplary use in further test reactions. This exploration can be used to categorically exclude *N*-oxides which were commonly an integral component of investigations and to consider others. These investigations are the key for a basic set of *N*-oxides which should not be neglected in a reaction optimization screening in homogeneous oxidative gold catalysis. The basic set of at least three *N*-oxides should include 2,5-dibromopyridine *N*-oxide, 2-trifluoromethylpyridine *N*-oxide and 8-methylquinoline *N*-oxide.

Experimental Section

General remarks

Chemicals were, if not noted otherwise, used from the stock of the University of Heidelberg or were bought from commercial suppliers such as Sigma-Aldrich, Strem and Carbolution. Deuterated solvents were purchased from Euriso-Top. The experiments were carried out in standard laboratory glassware.

NMR (Nuclear magnetic resonance) spectra were recorded at room temperature on Bruker Devices. The following instruments were available to choose from: Avance III-300 and Avance DRX-300. All chemical shifts δ were given in ppm and coupling constants *J* in Hz. ^{1}H and ^{13}C spectra were calibrated using the residual solvent signal ($CDCl_3$: 7.26 / 77.16 ppm; CD_2Cl_2: 5.32 / 53.84 ppm).

Gas Chromatography (GC) was processed on HP 58090 SERIES II with a HP 1 column. Nitrogen was used as the carrier gas.

General procedures

General procedure 1 (GP 1) – Synthesis of nitrogen coordinated gold(I)-complexes

A quoted amount of precatalyst $Ph_3PAuNTf_2$ (1.0 equiv) as well as pyridine derivative (1.0 equiv) were dissolved in dry DCM and stirred for 2 h at room temperature. The purity of the substances was taken into account when calculating the required amount of educts. Afterwards, the reaction mixture was filtered through Celite and the solvent was removed under reduced pressure. Finally, the residue was recrystallized from pentane.

General procedure 2 (GP 2) – Requirement for GC observed kinetic studies

The internal standard (IS) *n*-dodecane (5.7 µl, 25.1 µmol, 1 equiv) and the analyte were dissolved in 1.0 ml DCM in various stochiometric ratios (*n*-dodecane/analyte, 1:1, 1:0.5, 1:0.25). After analyzing the samples by means of gas chromatography, the corresponding response factors were calculated according to the following formula.

$$\mathrm{RF}_{\mathrm{analyte}} = \frac{\mathrm{area}_{\mathrm{IS}} \cdot \mathrm{c}_{\mathrm{analyte}}}{\mathrm{area}_{\mathrm{analyte}} \cdot \mathrm{c}_{\mathrm{IS}}}$$

General procedure 3 (GP 3) – Kinetic studies – Cyclopropanation

2-Methylbut-3-yn-2-yl pivalate (27.6 µl, 150.9 µmol, 1 equiv), styrene (69.2 µl, 603.7 µmol, 4 equiv) and the internal standard *n*-dodecane (34.3 µl, 150.9 µmol, 1 equiv) were dissolved in 2.0 ml dry DCM and stirred with a speed of 400 rpm. After addition of the nitrogen coordinated gold(I) complex, samples of the reaction mixture were taken in time intervals adjusted to the reaction rate. Separation of the catalyst was achieved by filtration through a short column of silica gel (PE/EA, 1:1). Then, the samples were analyzed by means of gas chromatography.

Note: In case of *in situ* activation, the precatalyst $Ph_3PAuNTf_2$ and the corresponding pyridine derivative were dissolved in 2.0 ml dry DCM and stirred with a speed of 400 rpm for 1 h at room temperature. Then, styrene and internal standard, *n*-dodecane, were added. After addition of the 2-methylbut-3yn-2-yl pivalate, samples of the reaction mixture were taken as described in the general procedure (GP 3).

General procedure 4 (GP 4) – Synthesis of *N*-oxides

The quoted amount of N-derivative (1 equiv) was dissolved in dry DCM. After cooling to 0 °C, the calculated amount of m-CPBA (1.6 equiv) was added gradually. The reaction mixture was allowed to warm up to room temperature und stirred overnight. After complete conversion of the starting material, the solution was quenched with

saturated $NaHCO_3$-solution and 2M NaOH-solution. The aqueous layer was separated and extracted with DCM. The combined organic layers were dried over Na_2SO_4, filtrated and concentrated under reduced pressure. The crude product was purified by column chromatography.

General procedure 5 (GP 5) – Kinetic studies – Gold(I)-catalyzed oxazole synthesis

Phenylacetylene (0.30 mmol, 1 equiv), *N*-oxide (0.39 mmol, 1.3 equiv) and the internal standard (0.30 mmol, 1 equiv) were dissolved in 3.0 ml acetonitrile and stirred with a speed of 400 rpm at 60 °C. After addition of the gold(I) complex $Ph_3PAuNTf_2$ (0.015 mmol, 0.05 equiv), samples of the reaction mixture were taken in time intervals adjusted to the reaction rate. Separation of the catalyst was achieved by filtration through a short column of silica gel (PE/EA, 1:1). Then, the samples were analyzed by means of gas chromatography.

General procedure 6 (GP 6) – Kinetic studies – Gold(I)-catalyzed ring expansion

A NMR tube was charged with a solution of 4-hydroxy-4-(phenylethynyl)cyclohexa-2,5-dien-1-one (0.060 mmol, 1 equiv) and *N*-oxide (0.078 mmol, 1.3 equiv) in 0.6 ml D_2-dichloromethane. Afterwards, the quoted amount of $Ph_3PAuNTf_2$ (0.003 mmol, 0.05 equiv) was added. The reaction was observed at T = 25 °C by ^1H NMR kinetic for 12 h. Here, the equipment Avance DRX-300 of Bruker Devices was selected. Due to often varying relaxation times, the measurement period distinguishes from substance to substance. Calculations of the measured time interval Δt are based on Equation 1:

$$\Delta t = (DS + NS)(AQ + T1) \quad (1)$$

DS – number of dummy scans NS – number of scans;

AQ – acquisition time (observation period) T1 – spin-lattice relaxation time constant

References

[1] a) A. S. K. Hashmi, *Chem. Rev.* **2007**, *107*, 3180 – 3211; b) A. Arcadi, *Chem. Rev.* **2008**, *108*, 3266 – 3325; c) F. Gagosz, *Actualite Chimique* **2010**, *347*,12 – 19; d) P. Garcia, M. Malacria, C. Aubert, V. Gandon, L. Fensterbank, *ChemCatChem* **2010**, *2*, 493 – 497; e) M. Rudolph, A. S. K. Hashmi, *Chem. Soc. Rev.* **2012**, *41*, 2448 – 2462;

f) L. Liu, G. B. Hammond, *Chem. Soc. Rev.* **2012**, *41*, 3129 – 3139; g) D. Zhang, X. Tang, M. Shi, *Acc. Chem. Res.* **2014**, *47*, 913 – 924.

[2] a) L. Ye, W. He, L. Zhang, *J. Am. Chem. Soc.* **2010**, *132*, 8550 – 8551; b) B. Lu, C. Li, L. Zhang, *J. Am. Chem. Soc.* **2010**, *132*, 14070 – 14072.

[3] a) J. Xiao, X. Li, *Angew. Chem. Int. Ed.* **2011**, *50*, 7226 – 7236; *Angew. Chem.* **2011**, *123*, 7364 – 7375; b) A. S. K. Hashmi, F. D. Toste, *Modern Gold Catalyzed Synthesis*, Wiley-VCH, 1st edn., **2012**; c) L. Zhang, *Acc. Chem. Res*. **2014**, *47*, 877 – 888; d) L. Ye, L. Zhang, *Synthesis of Oxygenated and Nitrogen-Containing Heterocycles by Gold-Catalyzed Alkyne Oxidation*; in: M. Bandini, *Au-Catalyzed Synthesis and Functionalization of Heterocycles*, Springer, 1st edn., **2016**.

[4] a) M. R. Fructos, T. R. Belderrain, P. de Frémont, N. M. Scott, S. P. Nolan, M. M. Díaz-Requejo, P. J. Pérez, *Angew. Chem. Int. Ed.* **2005**, *44*, 5284 – 5288; *Angew. Chem.* **2005**, *117*, 5418 – 5422; b) A. Prieto, M. R. Fructos, M. M. Díaz-Requejo, P. J. Pérez, P. Pérez-Galán, N. Delpont, A. M. Echavarren, *Tetrahedron* **2009**, *65*, 1790 – 1793; c) V. V. Pagar, A. M. Jadhav, R.-S. Liu, *J. Org. Chem.* **2013**, *78*, 5711 – 5716; d) V. V. Pagar, R.-S. Liu, *Angew. Chem. Int. Ed.* **2015**, *54*, 4923 – 4926; *Angew. Chem.* **2015**, *127*, 5005 – 5008.

[5] G. Henrion, T. E. J. Chavas, X. Le Goff, F. Gagosz, *Angew. Chem. Int. Ed.* **2013**, *52*, 6277 – 6282; *Angew. Chem.* **2013**, *125*, 6397 – 6402.

[6] a) Y. Wang, K. Ji, S. Lan, L. Zhang, *Angew. Chem. Int. Ed.* **2012**, *51*, 1915 – 1918; *Angew. Chem.* **2012**, *124*, 1951 – 1954; b) A. S. K. Hashmi, T. Wang, S. Shi, M. Rudolph, *J. Org. Chem.* **2012**, *77*, 7761 – 7767.

[7] J. Schulz, J. Jašík, A. Gray, J. Roithová, *Chem. Eur. J.* **2016**, *22* , 9827 – 9834.

[8] a) S. E. Thwaite, A. Schier, H. Schmidbaur, *Inorg. Chim. Acta* **2004**, *357*, 1549 – 1557; b) P. de Frémont, N. Marion, S. P. Nolan, *J. Organomet. Chem.* **2009**, *694*, 551 – 560; c) W. Yuan, X. Dong, Y. Wei, M. Shi, *Chem. Eur. J.* **2012**, *18*, 10501 – 10505; d) S. Orbisaglia, B. Jacques, P. Braunstein, D. Hueber, P. Pale, A. Blanc, P. de Frémont, *Organometallics* **2013**, *32*, 4153 – 4164.

[9] 1859090 (**1k**), 1859091 (**1l**), 1859092 (**1n**) and 1859093 (**1r**) contain the supplementary crystallographic data for this paper. These data can be obtained free

of charge from The Cambridge Crystallographic Data Centre via www.ccdc.cam.ac.uk/data_request/cif.

[10] a) M. J. Johansson, D. J. Gorin, S. T. Staben, F. D. Toste*, J. Am. Chem. Soc.* **2005**, *127*, 18002 – 18003; b) J. Petuškova, H. Bruns, M. Alcarazo, *Angew. Chem. Int. Ed.* **2011**, *50*, 3799–3802; *Angew. Chem.* **2011**, *123*, 3883 – 3886.

[11] R. L. Grob, E. F. Barry, *Modern Practice of Gas Chromatography*, Wiley Interscience, Hoboken, NJ, 4th edn., **2005**.

[12] a) H. G. Elias, *Makromoleküle: Chemische Struktur und Synthesen*, Wiley-VCH, 6th edn., **1999**; b) W. Bechmann, J. Schmidt, *Einstieg in die Physikalische Chemie für Nebenfächler*, B. G. Teubner, 1st edn., **2001**; c) P. W. Atkins, J. Paula, *Physikalische Chemie*, Wiley-VCH, 4th edn., **2006**; d) P. L. Houston, *Chemical Kinetics and Reaction Dynamics*, Dover Publications, Inc., Minola, New York, **2012**.

[13] M. Lõkov, S. Tshepelevitsh, A. Heering, P. G. Plieger, R. Vianello, I. Leito, *Eur. J. Org. Chem.* **2017**, 4475 – 4489.

[14] a) D. Rong, V. A. Phillips, R. Sánchez Rubio, M. A. Castro, R. T. Wheelhouse, *Tetrahedron Lett.* **2008**, *49*, 6933 – 6935; b) G. Li, C. Jia, K. Sun, Y. Lv, F. Zhao, K. Zhou, H. Wu, *Org. Biomol. Chem.* **2015**, *13*, 3207 – 3210; c) J. Zhao, P. Li, C. Xia, F. Li, *RSC Adv.* **2015**, *5*, 32835 – 32838; d) X. Ma, H. Dang, J. A. Rose, P. Rablen, S. B. Herzon, *J. Am. Chem. Soc.* **2017**, *139*, 5998 – 6007.

[15] a) Y. Wang, K. Ji, S. Lan, L. Zhang, *Angew. Chem. Int. Ed.* **2012**, *51*, 1915 – 1918; *Angew. Chem.* **2012**, *124*, 1951 – 1954; b) M. Butler, G. M. Cabrera, *J. Mol. Struct.* **2013**, *1043*, 37 – 42; c) H. Hwang, J. Kim, J. Jeong, S. Chang, *J. Am. Chem. Soc.* **2014**, *136*, 10770 – 10776; d) C. Zhu, M. Yi, D. Wei, X. Chen, Y. Wu, X. Cui, Org. Lett. 2014, 16, 1840 – 1843.

[16] W. Yang, R. Zhang, F. Yi, M. Cai, *J. Org. Chem.* **2017**, *82*, 5204 − 5211.

[17] N. V. Belova, N. I. Giricheva, M. S. Fedorov, *Struct. Chem.* **2015**, DOI: 10.1007/s11224-015-0621-9.

[18] J. Zhao, J. Liu, X. Xie, S. Li, Y. Liu, *Org. Lett.* **2015**, *17*, 5926 − 5929.

[19] P. Nösel, S. Moghimi, C. Hendrich, M. Haupt, M. Rudolph, F. Rominger, A. S. K. Hashmi, *Adv. Synth. Catal.* **2014**, *356*, 3755 – 3760.

[20] a) C. Khin, A. S. K. Hashmi, F. Rominger, *Eur. J. Inorg. Chem.* **2010**, 1063-1069; b) L. Huang, M. Rudolph, F. Rominger, A. S. K. Hashmi, *Angew. Chem. Int. Ed.* **2016**, *55*, 4808-4813; *Angew. Chem.* **2016**, *128*, 4888-4893; c) L. Huang, F. Rominger, M. Rudolph, A. S. K. Hashmi, *Chem. Commun.* **2016**, *52*, 6435-6438.

.

TOC graphic